

# Dynamics of Photoinduced Electron Transfer in a Carotenoid–Porphyrin–Dinitronaphthalenedicarboximide Molecular Triad

Quan Tan, Darius Kuciauskas, Su Lin, Simon Stone, Ana L. Moore,\* Thomas A. Moore,\* and Devens Gust\*

Center for the Study of Early Events in Photosynthesis, Department of Chemistry and Biochemistry, Arizona State University, Tempe, Arizona 85287-1604

Received: February 25, 1997; In Final Form: April 22, 1997<sup>⊙</sup>

An electron acceptor moiety based on the 4,5-dinitro-1,8-naphthalenedicarboximide system has been prepared and used as the basis for synthesis of a porphyrin–imide dyad (P–NIm) and a carotenoid–porphyrin–imide triad molecule (C–P–NIm). Excitation of the porphyrin moiety in either compound with visible light leads to rapid photoinduced electron transfer to generate in high yield a charge-separated state consisting of the porphyrin radical cation and imide radical anion. In the triad, this C–P<sup>•+</sup>–NIm<sup>•-</sup> state decays in part by a second electron transfer from the carotenoid to yield a final C<sup>•+</sup>–P–NIm<sup>•-</sup> charge-separated state. In benzonitrile, this state is formed with a quantum yield of 0.33 and has a lifetime of 430 ns. The 4,5-dinitro-1,8-naphthalenedicarboximide moiety is conveniently synthesized and undergoes facile and reversible one-electron reduction. The NIm<sup>•-</sup> ion has a readily observable spectroscopic signature in the visible. In contrast to a series of closely related triads reported by other investigators, the triad studied here shows no evidence for photoinduced electron transfer from the carotenoid first excited singlet state.

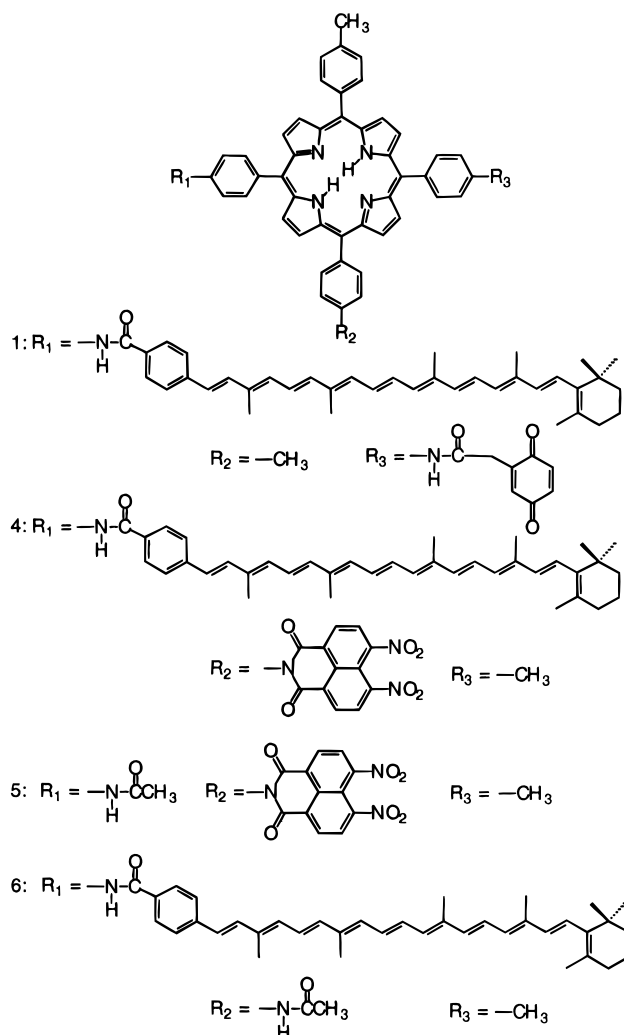
## Introduction

Dyads, triads, and other multicomponent supermolecules consisting of covalently linked chromophores and electron donors and acceptors have proven useful as mimics of photosynthetic reaction centers, which convert light energy into chemical potential via energy transfer and photoinduced electron-transfer processes.<sup>1–6</sup> In principle, such molecules can also be made to function as molecular-scale optoelectronic switches and logic elements.<sup>7–9</sup> A typical system of this type is a donor–pigment–acceptor triad such as carotenoid–porphyrin–quinone (C–P–Q) triad **1** (see Chart 1) first reported by our group 14 years ago.<sup>10,11</sup> The porphyrin pigment absorbs light, and its first excited singlet state, C–<sup>1</sup>P–Q, donates an electron to the quinone acceptor to form C–P<sup>•+</sup>–Q<sup>•-</sup>. This state evolves by electron transfer from the carotenoid secondary electron donor to yield a final C<sup>•+</sup>–P–Q<sup>•-</sup> charge-separated state. The final state lives for microseconds, is formed with a reasonable quantum yield, and preserves a substantial fraction of the photon energy as chemical potential. The key to the function of this triad is the two-step electron-transfer sequence, which allows formation of the final charge-separated state in high yield but electronically and energetically separates the oxidizing and reducing elements to retard charge recombination to the ground state.

In photosynthesis, quinones perform useful roles in electron and proton transport, but they are not the primary electron acceptors in the photoinduced electron-transfer reaction. In artificial systems, other electron acceptors including porphyrins, fullerenes,<sup>12–18</sup> and aromatic imides<sup>19–34</sup> have proven useful in dyad, triad, and more complex devices. Imide acceptors can be more chemically robust than quinones and can be linked to other molecules in ways that limit conformational mobility. In some cases, their radical anions have characteristic absorption spectra that allow relatively easy spectroscopic detection.

Synthetic and photophysical studies of an interesting series of triad molecules consisting of porphyrins covalently linked to carotenoids and pyromellitimide (Im) moieties have recently

CHART 1: Structures 1, 4–6



been reported by Osuka, Mataga, and co-workers.<sup>27</sup> Excitation of the carotenoid moiety of C–P–Im triads **2** and **3** (Chart 2)

<sup>⊙</sup> Abstract published in *Advance ACS Abstracts*, June 1, 1997.

## CHART 2: Structures 2 and 3

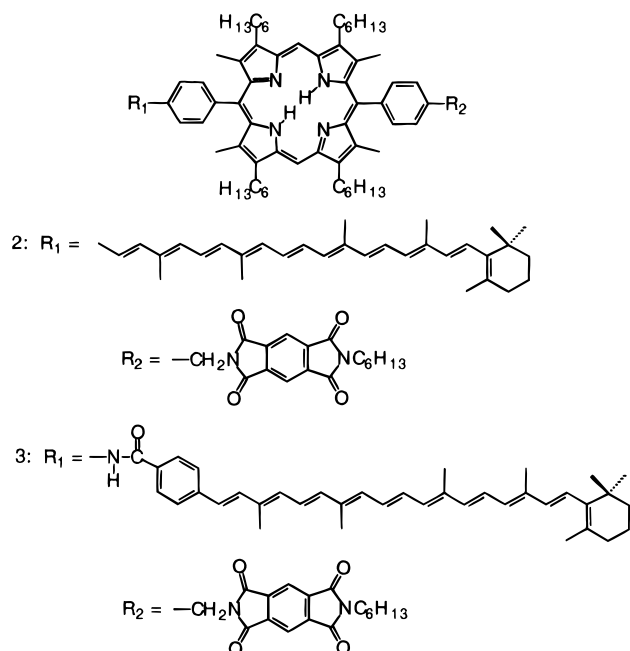
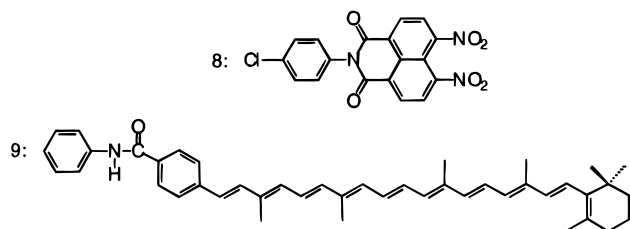


## CHART 3: Structures 8 and 9



was found to initiate photoinduced electron transfer from the carotenoid first excited singlet state,  $^1C-P-Im$ , to yield  $C^{+}-P-Im^{-}$  in a direct, one-step electron-transfer reaction. Excitation of the porphyrin moiety of **2** was followed by rapid singlet-singlet energy transfer to the carotenoid to give  $^1C-P-Im$ , which then evolved directly to the  $C^{+}-P-Im^{-}$  charge-separated state. The authors thus suggested the single-step, long-range charge separation mechanism as an alternative to the two-step mechanism proposed for the quinone-containing triads.

To investigate the generality of the intriguing single-step long-range electron transfer observed in the C-P-Im triads, we initially studied the photochemistry of several C-P-Q triads and found no evidence for significant photoinduced electron transfer from the carotenoid first excited singlet state.<sup>35</sup> Now we turn our attention to triads with imide-based electron acceptor moieties. We report the preparation of triad **4** and model compounds **5**, **6**, **8** and **9** (Charts 1 and 3), electrochemical investigations of these compounds, and the study of their photochemical properties using time-resolved absorption and emission techniques. Note that **4** includes a carotenoid moiety with an amide link to the porphyrin *meso*-aryl ring similar to that in **1** and **3**. The acceptor is a 4,5-dinitro-1,8-naphthalene-2,3-dicarboximide (NIm). This electron acceptor has the structural advantages of pyromellitimides such as that in **2** and **3**, but is more easily reduced (see below), and can therefore serve as an effective acceptor under a wider variety of conditions.

## Results

**Synthesis.** The porphyrin and carotenoid moieties of **4** were prepared as previously described. Nitration of commercially available 4-nitronaphthalic anhydride yielded the 4,5-analogue,

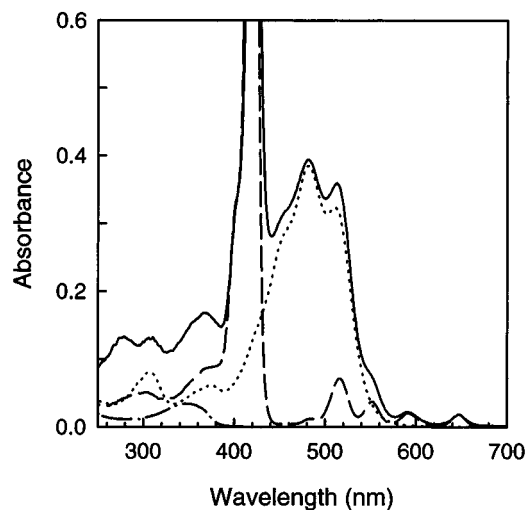


**Figure 1.** Absorption spectra of triad **4** (—), porphyrin **7** (---), imide **8** (- · -), and carotenoid **9** (···) in dichloromethane solution. The porphyrin Soret band is truncated.

which was coupled with the appropriate porphyrin to produce a P-NIm dyad. Reaction with the acid chloride of the requisite carotenoid yielded **4**. The model compounds were prepared using related methods, as described in the Experimental Section.

**Electrochemical Studies.** Cyclic voltammetric studies of model imide **8** in benzonitrile solution gave two reversible reductions at  $-0.88$  and  $-1.20$  V vs ferrocene/ferrocenium as an internal reference. The first one-electron reduction potential of the imide moiety of **2** is  $-1.24$  V.<sup>32</sup> The first oxidation potential of a model for the porphyrin moiety of **4** is  $+0.47$  V in benzonitrile, whereas the carotenoid is oxidized at  $+0.18$  V (determined in dichloromethane).<sup>36</sup>

**Steady-State Absorption Spectra.** The absorption spectra of triad **4**, *meso*-tetraphenylporphyrin (**7**), model imide **8**, and model carotenoid **9** in dichloromethane are shown in Figure 1. Porphyrin **7** exhibits a Soret absorption at 417 nm and Q-bands at 516, 552, 591, and 647 nm. The carotenoid moiety has major absorption maxima at 450 (sh), 481, and 513 nm. The imide absorptions are found in the 250–380 nm region. The spectrum of the triad is similar to a linear combination of the spectra of the component chromophores. Thus, the absorption spectrum shows no indication of strong electronic interactions between the various pigments. In polar solvents such as benzonitrile, all absorption bands are shifted to longer wavelengths by 1–8 nm.

**Fluorescence Spectra.** The fluorescence emission spectra of triad **4** and dyad **5** in benzonitrile solution, with excitation at 590 nm, are similar in shape to that of model porphyrin **7** with maxima at 656 and 721 nm, but the fluorescence quantum yields are much lower than that of **7** (see next paragraph). The fluorescence excitation spectrum of **4** in the 430–700 nm region, with detection at 720 nm, is nearly identical with that of model porphyrin **7**, with little or no contribution from light absorbed by the carotenoid polyene. From these results, it can be calculated that singlet-singlet energy transfer from the carotenoid to the porphyrin is  $<10\%$  efficient.

The strong porphyrin fluorescence quenching observed for **4** and **5** indicates that attachment of the carotenoid and imide moieties to the porphyrin provides new pathways for deactivation of the porphyrin first excited singlet state. Quantitative information concerning the quenching was obtained from time-resolved fluorescence studies using the single-photon timing technique, with excitation at 590 nm. The lifetime of the first excited singlet state of porphyrin **7** in benzonitrile is 9.7 ns.

**TABLE 1: Time Constants for Photochemical Processes in Triad 4 and Model Dyads**

solvent	$\epsilon^a$	dyad 5			dyad 6		triad 4		
		$\tau_S^b$ (ps)	$\tau_R$ (ps)	$\tau_D$ (ps)	$\tau_S^b$ (ns)	$\tau_S^b$ (ps)	$\tau_R^g$ (ps)	$\tau_D^h$ (ns)	
toluene	2.4	116	124 <sup>c</sup>	807 <sup>e</sup>	3.70	110	NO	NO	
ethyl acetate	6.0	432						190	
2-methyltetrahydrofuran	7.6	264	12.7 <sup>d</sup>	240 <sup>f</sup>	3.48	243		173	
dichloromethane	8.9	60			3.00	59		340	
benzonitrile	25.2	103	12.9 <sup>d</sup>	107 <sup>f</sup>	2.21	93	99	430	

<sup>a</sup> Dielectric constant from ref 44. <sup>b</sup> Lifetime of the porphyrin first excited singlet state measured by time-resolved fluorescence techniques. <sup>c</sup> Rise time of transient absorbance corresponding to formation of  $P^{*+}-NIm^{*-}$ . <sup>d</sup> Rise time of transient absorbance corresponding to decay of  $P^{*+}-NIm^{*-}$  (see text). <sup>e</sup> Decay time of  $P^{*+}-NIm^{*-}$  measured by subpicosecond transient absorption techniques. <sup>f</sup> Decay time of transient absorbance corresponding to decay of the porphyrin first excited singlet state and concurrent formation of  $P^{*+}-NIm^{*-}$ . <sup>g</sup> Rise time of the carotenoid radical cation measured by subpicosecond transient absorption techniques. <sup>h</sup> Decay time of the carotenoid radical cation measured by nanosecond transient absorption techniques.

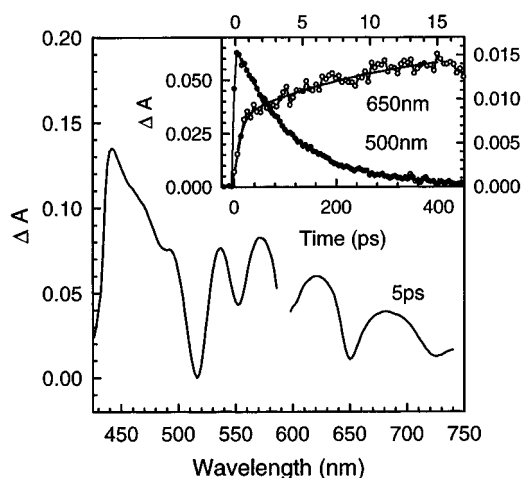


**Figure 2.** Transient absorption spectrum of dyad 5 in benzonitrile taken 5 ps after excitation with a 200 fs, 590 nm laser pulse. The spectrum is an average of several thousand experiments. The inset shows the rise of the transient absorption at 650 nm and the corresponding two-exponential fit to time constants of 400 fs and 12.9 ps (top and right axes). Also shown in the inset is the decay of the transient at 500 nm and the corresponding fit with a time constant of 107 ps (bottom and left axes).

The fluorescence decay of carotenoporphyrin 6 was measured in benzonitrile at seven wavelengths in the 640–750 nm region and the results analyzed globally ( $\chi^2 = 1.04$ ). The only significant decay component has a lifetime of 2.2 ns. Thus, the carotenoid quenches the porphyrin first excited singlet state. This state is quenched even more strongly by the imide moiety. The emission decays for porphyrin–imide dyad 5 were measured in benzonitrile at five wavelengths in the 650–740 nm region. Global analysis ( $\chi^2 = 1.10$ ) yielded a single significant decay component with a lifetime of 103 ps for  $^1P-NIm$ . Similar experiments with triad 4 gave a lifetime for  $C-^1P-NIm$  of 93 ps (global analysis at seven wavelengths in the 640–750 nm region,  $\chi^2 = 1.07$ ). Fluorescence lifetimes were also determined in toluene, ethyl acetate, 2-methyltetrahydrofuran, and dichloromethane. In all cases, satisfactory goodness-of-fit parameters were obtained, and only one significant decay component was observed. The lifetimes are listed in Table 1.

**Picosecond Transient Absorption Experiments.** The strong quenching of the porphyrin first excited singlet state of  $P-NIm$  dyad 5 noted above suggests photoinduced electron transfer to yield  $P^{*+}-NIm^{*-}$ , as has been observed for a variety of other porphyrin–imide dyads. This possibility was investigated using transient absorption techniques. Figure 2 shows the transient absorption spectrum of 5 in benzonitrile solution obtained 5 ps after excitation at 590 nm (where only the porphyrin moiety absorbs) with a  $\sim 200$  fs laser pulse, averaged over several hundred thousand laser flashes. No significant sample decom-

position was observed during these experiments. There is a net transient absorption increase over the whole 450–750 nm region due to absorption by the porphyrin first excited singlet state. Spectral minima at 516, 552,  $\sim 590$ , and 650 nm correspond to porphyrin ground-state absorption (Figure 1) and represent depletion of the ground state. Stimulated emission from the porphyrin is observed as minima at 650 and 726 nm, corresponding to porphyrin fluorescence bands. Thus, at 5 ps, the transient absorption spectrum is essentially that of the first excited singlet state of the porphyrin moiety.

The inset in Figure 2 shows the transient absorption kinetics at 500 and 650 nm measured on different time scales. At 500 nm, where absorption by the porphyrin first excited singlet state is strong, the transient absorbance decays monoexponentially with a time constant of 107 ps. This is equal to the 103 ps lifetime of  $^1P-NIm$  determined from the single-photon timing fluorescence measurements, within experimental error. Figure 2 shows that at 650 nm, the net absorption change resulting from excitation of the porphyrin to its first excited singlet state is nearly zero. Thus, the kinetic behavior of states with smaller contributions to the transient absorption spectrum can be observed at this wavelength. On a short time scale, the rise of the transient absorption at 650 nm is biexponential with lifetimes of  $\sim 400$  fs and 12.9 ps. The time constant for decay of the absorbance is again  $\sim 100$  ps. The 400 fs rise is ascribed to formation of  $^1P-NIm$  with the laser pulse, and the decay of the transient at 650 nm (not shown) is due to the decay of  $^1P-NIm$ , as confirmed by the time-resolved fluorescence measurements. The decay of  $^1P-NIm$  is attributed to photoinduced electron transfer to yield the  $P^{*+}-NIm^{*-}$  charge-separated state, which is therefore formed with a time constant of 100 ps.

The 12.9 ps rise time of the transient absorption at 650 nm is actually associated with the decay of the  $P^{*+}-NIm^{*-}$  charge-separated state. The time constant for decay of the charge-separated species appears as a rise time in the transient absorption experiment because the rate constant for charge recombination of  $P^{*+}-NIm^{*-}$  to the ground state is larger than that for its formation from  $^1P-NIm$ . Related kinetic behavior has been observed in dyads consisting of porphyrins linked to quinone acceptors.<sup>35</sup> Similar transient absorption experiments were carried out in 2-methyltetrahydrofuran and in toluene. The results are tabulated in Table 1. It will be noted that in toluene, the lifetime of the  $P^{*+}-NIm^{*-}$  state is  $\sim 7$  times longer than that of  $^1P-NIm$ , and normal kinetic behavior is observed.

Figure 3 shows picosecond transient absorption spectra obtained from benzonitrile solutions of triad 4 after excitation at 590 nm with a  $\sim 200$  fs laser pulse. The spectrum obtained 5 ps after excitation is characteristic of the porphyrin first excited singlet state, with minima at 650 and  $\sim 720$  nm due to ground-state depletion and stimulated emission (see Figure 2). At 300 ps after excitation, the signature of the excited singlet state is

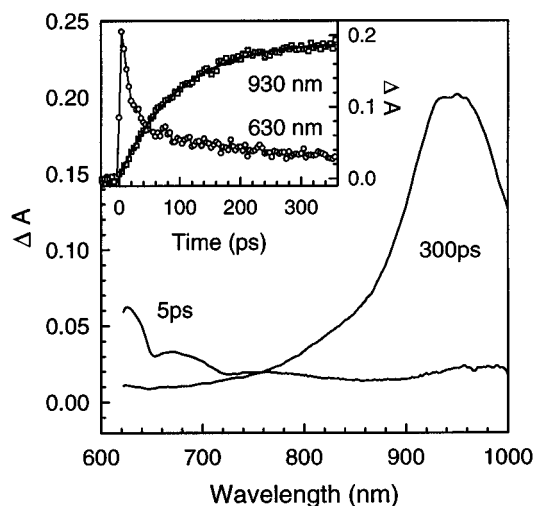


**Figure 3.** Transient absorption spectra of triad **4** in benzonitrile taken 5 and 300 ps after excitation with a 200 fs, 590 nm laser pulse. The inset shows the rise of the carotenoid radical cation absorption at 930 nm with a time constant of 99 ps and the decay of the transient absorbance at 630 nm, which includes three exponential components (see text).

absent, and the spectrum is dominated by a strong absorption in the 850–1000 nm region that is characteristic of the carotenoid radical cation.<sup>36</sup> This transient represents the  $C^{+}-P-NIm^{-}$  charge-separated state.

The inset in Figure 3 shows the transient absorption kinetics measured at 630 and 930 nm. Global analysis of the data in the 850–1032 nm region demonstrated that the carotenoid radical cation absorption rises from zero as a single exponential with a time constant of 99 ps (Table 1). The absorption does not decay on the subnanosecond time scale. Global analysis of the data in the 604–750 nm region, taken on different time scales, showed that the decay is best fit by three exponential components: 7.7 ps (80%), 99 ps (14%), and  $>1$  ns (6%). The spectrum for the 7.7 ps component has a maximum at 624 nm, and this spectrum and the lifetime indicate that this component is due to the carotenoid first excited singlet state. The carotenoid transient absorption arises because the carotenoid is responsible for about 10% of the total excitation light absorption at 590 nm. The 99 ps component has the spectrum of the porphyrin first excited singlet state, and its lifetime is the same as that determined for  $C^{-1}P-Q$  by time-resolved fluorescence spectroscopy. The small, long-lived component ( $\tau > 1$  ns) is due to the  $NIm$  radical anion, as discussed below.

Picosecond transient absorption experiments were also performed with excitation at 556 nm, where the carotenoid is responsible for 43% of the total light absorption. Global analysis of the data in the 850–992 nm region showed that the rise of the carotenoid radical cation was again a single exponential with a time constant of 99 ps. No formation of carotene radical cation with a time constant in the 7.7 ps range was observed.

Picosecond transient absorption experiments with excitation at 590 nm were also carried out in 2-methyltetrahydrofuran solution, and the relevant time constants appear in Table 1. Experiments were performed in toluene solution, but no carotenoid radical cation was observed under these conditions.

**Nanosecond Transient Absorption Experiments.** Excited-state dynamics on a longer time scale were investigated using nanosecond transient absorption spectroscopy. Figure 4 shows the decay of the carotenoid radical cation absorption of the  $C^{+}-P-NIm^{-}$  state following excitation of triad **4** in various deoxygenated solvents at 650 nm with a  $\sim 5$  ns laser pulse. The

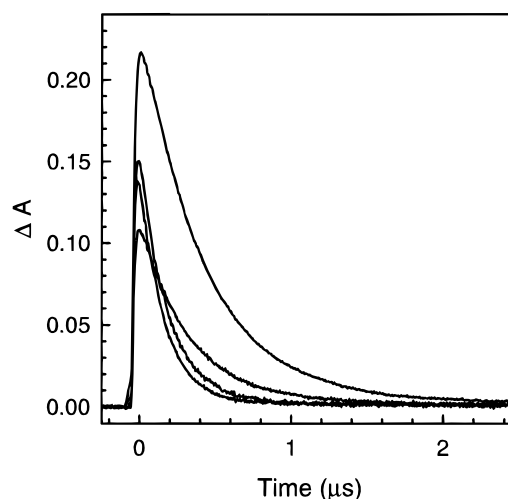


**Figure 4.** Decay of the transient absorbance of the carotenoid radical cation of the  $C^{+}-P-NIm^{-}$  charge-separated state following excitation with a  $\sim 5$  ns, 650 nm laser pulse. The decays were measured at the maxima of the radical cation absorptions. The decays, in order of decreasing maximum amplitude, were obtained in benzonitrile, ethyl acetate, 2-methyltetrahydrofuran, and dichloromethane and represent samples with equal absorbance at the excitation wavelength.

maximum of the carotenoid radical cation absorption is solvent dependent and occurs at 920 nm in ethyl acetate, 930 nm in 2-methyltetrahydrofuran, 960 nm in dichloromethane, and 950 nm in benzonitrile. The decay of the carotenoid radical cation due to charge recombination is a single-exponential process; the lifetimes are 190 ns in ethyl acetate, 173 ns in 2-methyltetrahydrofuran, 340 ns in dichloromethane, and 430 ns in benzonitrile. Quantum yields for the  $C^{+}-P-NIm^{-}$  state in the various solvents were determined from linear regression analyses of the dependence of the amplitude of the carotenoid radical cation transient absorption ( $\epsilon = 1.6 \times 10^5 \text{ L mol}^{-1} \text{ cm}^{-1}$ ) on excitation intensity, using the triplet state of porphyrin **7** as a standard ( $\phi_T = 0.67$ ,  $(\epsilon_T - \epsilon_G)_{440} = 6.8 \times 10^4 \text{ L mol}^{-1} \text{ cm}^{-1}$ ). The quantum yields were 0.23, 0.20, 0.16, and 0.33 for ethyl acetate, 2-methyltetrahydrofuran, dichloromethane, and benzonitrile, respectively.

With 650 nm excitation, only the porphyrin first excited singlet state is produced. Triad **4** in 2-methyltetrahydrofuran was also excited at 550 nm, where the carotenoid moiety absorbs 60% of the light. Under these conditions, the quantum yield of  $C^{+}-P-NIm^{-}$  was only  $\sim 9\%$ . This yield can be attributed to light absorbed by the porphyrin, in accord with the results from 650 nm excitation discussed above; excitation of the carotenoid moiety does not lead to significant ( $> 1\%$ ) formation of the  $C^{+}-P-NIm^{-}$  charge-separated state.

Nanosecond transient absorption measurements of solutions of **4** in deoxygenated benzonitrile with 650 nm excitation were also performed in the 550–580 nm spectral region (Figure 5). The kinetics at 550 nm feature the prompt appearance of an absorbance decrease, which recovers with a 430 ns time constant superimposed on a much weaker decay component of 4.4  $\mu\text{s}$ . The 430 ns component of the decay is not sensitive to oxygen, has the lifetime of the carotenoid radical cation, and is assigned to recovery from the carotenoid ground-state bleaching as  $C^{+}-P-NIm^{-}$  decays back to the ground state. The 4.4  $\mu\text{s}$  component is due to the carotenoid triplet state, as shown by its spectrum, which is shown 2  $\mu\text{s}$  after excitation as an inset in Figure 5. The component is quenched by oxygen, as expected for this triplet state. The quantum yield of  ${}^3C-P-NIm$  is  $\sim 0.03$ . Formation of  ${}^3C-P-NIm$  is ascribed to triplet-triplet energy transfer from  $C-{}^3P-NIm$ , which is generated by normal intersystem crossing. Consistent with this interpretation is the

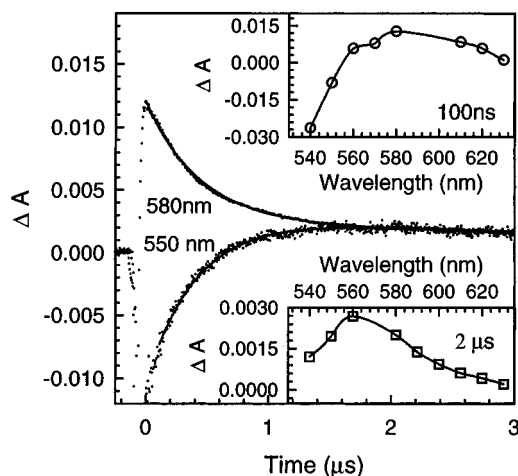


**Figure 5.** Transient absorption kinetics of triad **4** in benzonitrile measured after excitation with a  $\sim 5$  ns, 650 nm laser pulse. The solid lines show multiexponential fits to the data at 580 nm (430 ns and 4.4  $\mu$ s decay times) and 550 nm (430 ns rise, 4.4  $\mu$ s decay). The insets show the transient absorption spectra measured 100 ns and 2  $\mu$ s after excitation.

fact that in 2-methyltetrahydrofuran the yield of  ${}^3\text{C-P-NIm}$  increases to  $\sim 0.09$ . This increase is due to the increased lifetime of  $\text{C}^+-\text{P-NIm}$  in this solvent (Table 1) and thus a higher yield of  $\text{C}^+-\text{P-NIm}$  (Table 2).

The absorption decay at 580 nm following excitation in benzonitrile can be fitted with two exponential components of 430 ns (79%) and 4.4  $\mu$ s (21%). The 4.4  $\mu$ s component is quenched by oxygen and is assigned to  ${}^3\text{C-P-NIm}$  as discussed above. The spectrum of the 430 ns decay component taken 100 ns after excitation (Figure 5) and its lifetime suggest that it arises from the  $\text{NIm}^{\bullet-}$  moiety of the  $\text{C}^+-\text{P-NIm}^{\bullet-}$  charge-separated state superimposed on carotenoid ground-state bleaching. The spectrum of the radical anion of model imide **8**, generated electrochemically, features absorption in the 500–650 nm region with a broad maximum at 520 nm (Figure 6). Comparison of the transient absorbance at 580 nm with that of the carotenoid radical cation at 950 nm ( $\epsilon_{950} = 1.6 \times 10^5 \text{ L mol}^{-1} \text{ cm}^{-1}$ ) allows a rough estimation of the extinction coefficient of  $\text{NIm}^{\bullet-}$  as  $\sim 2.2 \times 10^4 \text{ L mol}^{-1} \text{ cm}^{-1}$  at 580 nm. This estimate in turn may be used to calculate an extinction coefficient of  $\sim 3.4 \times 10^4 \text{ L mol}^{-1} \text{ cm}^{-1}$  for  $\text{NIm}^{\bullet-}$  at its 520 nm absorption maximum, which is obscured by carotenoid ground-state bleach in the spectrum of triad **4**. In aerated samples, the lifetime of the 580 nm decay is reduced by a factor of up to 2, depending upon the oxygen concentration. This likely signals some reaction of  $\text{NIm}^{\bullet-}$  with molecular oxygen.

## Discussion

**Photoinduced Electron Transfer from the Porphyrin First Excited Singlet State.** We will first discuss the spectroscopic results obtained from excitation of the porphyrin moiety in benzonitrile solution. The first excited singlet state of model porphyrin **7** has a lifetime of 9.7 ns in this solvent and decays by intersystem crossing to the triplet, fluorescence, and internal conversion. Attaching the imide moiety, as in dyad **5**, reduces the lifetime of the porphyrin first excited singlet state,  $\tau_s$ , to 105 ps (Table 1) by introducing a new decay pathway: photoinduced electron transfer to the attached  $\text{NIm}$  moiety to yield  $\text{P}^+-\text{NIm}^{\bullet-}$ . (The lifetime noted here is an average of the 103 ps lifetime measured by fluorescence techniques and the 107 ps lifetime determined by transient absorption.) The rate constant for photoinduced electron transfer,  $k_{cs}$ , is given by eq 1, where  $k_m$  is the reciprocal of the 9.7 ns lifetime of the

first excited singlet state of model porphyrin **7**;  $k_{cs}$  equals  $9.4 \times 10^9 \text{ s}^{-1}$ .

$$k_{cs} = \left( \frac{1}{\tau_s} \right) - k_m \quad (1)$$

The quantum yield of  $\text{P}^+-\text{NIm}^{\bullet-}$  ( $\tau_s k_{cs}$ ) equals 0.99. The  $\text{P}^+-\text{NIm}^{\bullet-}$  state recombines to the ground state in 12.9 ps, with  $k_{cr} = 7.8 \times 10^{10} \text{ s}^{-1}$ . The fact that charge recombination is more rapid than charge separation gives rise to the “inverse kinetic” spectroscopic behavior discussed above. Rate constants for charge separation and recombination in benzonitrile and other solvents appear in Table 2.

Turning to triad **4**, the kinetic behavior in benzonitrile may be discussed with reference to Figure 7, which shows the relevant high-energy states and their interconversion pathways. The energies of the excited states have been estimated from spectroscopic data, and the energies of the charge-separated states are based on the cyclic voltammetric results presented above. No corrections for Coulombic effects have been made.

Excitation of the porphyrin moiety, as was achieved by 650 nm laser pulses, produces  $\text{C}^+-\text{P-NIm}$ , which decays in 96 ps (an average of the 93 ps lifetime from fluorescence studies and the 99 ps lifetime from transient absorption measurements.) In the absence of the imide acceptor, the lifetime of the porphyrin first excited singlet state is 2.21 ns, as determined from studies of model carotenoporphyrin **6**. Thus,  $k_1$ , the rate constant for step 1 in Figure 7, may be estimated as  $4.5 \times 10^8 \text{ s}^{-1}$ . The drastic shortening of the lifetime of the porphyrin first excited singlet state upon introduction of the imide moiety is due to photoinduced electron-transfer step 2, which yields  $\text{C-P}^+-\text{NIm}^{\bullet-}$ . Calculation analogous to that indicated in eq 1 yields  $k_2 = 1.0 \times 10^{10} \text{ s}^{-1}$ , which is close to the rate constant obtained for photoinduced electron transfer in dyad **5**. The quantum yield of  $\text{C-P}^+-\text{NIm}^{\bullet-}$ ,  $\Phi_2$ , is 0.96.

The intermediate  $\text{C-P}^+-\text{NIm}^{\bullet-}$  state decays by two routes: charge recombination to the ground state (step 3) and electron transfer from the carotenoid to give the final  $\text{C}^+-\text{P-NIm}^{\bullet-}$  species (step 4). The overall quantum yield of  $\text{C}^+-\text{P-NIm}^{\bullet-}$ ,  $\Phi_{\text{C}^+-\text{P-NIm}^{\bullet-}}$ , was measured to be 0.33 and is given by eq 2:

$$\Phi_{\text{C}^+-\text{P-NIm}^{\bullet-}} = \Phi_2 \frac{k_4}{k_3 + k_4} \quad (2)$$

If we estimate  $k_3$  as  $7.8 \times 10^{10} \text{ s}^{-1}$ , as was found for model dyad **5**, then  $k_4 = 4.1 \times 10^{10} \text{ s}^{-1}$ . The final  $\text{C}^+-\text{P-NIm}^{\bullet-}$  state decays to the ground state with  $k_5 = 2.3 \times 10^6 \text{ s}^{-1}$ . Rate constants for some steps in Figure 7 may be calculated from the time-resolved data in other solvents using these same considerations. The results are given in Table 2.

**Photoinduced Electron Transfer from a Carotenoid Excited Singlet State.** Several of the experiments described above bear on the question of possible photoinduced electron transfer from  ${}^1\text{C-P-NIm}$  to yield the final  $\text{C}^+-\text{P-NIm}^{\bullet-}$  state. When triad **4** is excited at 590 nm, where the carotenoid absorbs 10% of the light, the picosecond transient absorption experiments show that the carotenoid first excited singlet state absorption is readily observable and has a lifetime of 7.7 ps (Figure 3). The lifetime of the unperturbed first excited singlet state of a carotenoid such as that in **4** is  $\sim 10$  ps.<sup>27,38</sup> Thus, quenching of the carotenoid first excited singlet state by the porphyrin or imide moieties of the triad must be minimal. In addition, any such quenching that was due to photoinduced electron transfer must

TABLE 2: Rate Constants and Quantum Yields for Photochemical Processes in Dyad 5 and Triad 4

solvent	dyad 5							triad 4			
	$\epsilon^a$	$k_{es}^b$ $\times 10^{-9}$ $s^{-1}$	$k_{cr}^c$ $\times 10^{-9}$ $s^{-1}$	$k_1^d$ $\times 10^{-9}$ $s^{-1}$	$k_2^e$ $\times 10^{-9}$ $s^{-1}$	$k_3^f$ $\times 10^{-9}$ $s^{-1}$	$k_4^g$ $\times 10^{-9}$ $s^{-1}$	$k_5^h$ $\times 10^{-9}$ $s^{-1}$	$\Phi_{C-P^+-NIm^{*-}}$	$\Phi_{C^{*+}-P-NIm^{*-}}$	$\Phi_{C-P-NIm}^3$
toluene	2.4	8.5	1.2	0.27	8.8	1.2	NO	NO	0.97	NO	0.02
ethyl acetate	6.0	2.2						5.3		0.23	
2-methyltetrahydrofuran	7.6	3.7	79	0.29	3.8	79	22	5.8	0.92	0.20	0.09
dichloromethane	8.9	16.6		0.33	16.6			2.9	0.98	0.16	0.02
benzonitrile	25.2	9.4	78	0.45	10.0	78	41	2.3	0.96	0.33	0.03

<sup>a</sup> Dielectric constant from ref 44. <sup>b</sup> Determined from the lifetime of the porphyrin first excited singlet state using eq 1. <sup>c</sup> Determined from subpicosecond transient absorption results. <sup>d</sup> Estimated from the lifetime of the porphyrin first excited singlet state of carotenoporphyrin **6** as determined from time-resolved fluorescence studies. <sup>e</sup> Determined from the lifetime of the porphyrin first excited singlet state using an equation analogous to eq 1. <sup>f</sup> Estimated from corresponding rate in dyad **5**. <sup>g</sup> Calculated according to eq 2. <sup>h</sup> Calculated from the lifetime of the carotenoid radical cation as determined by nanosecond transient absorption spectroscopy.

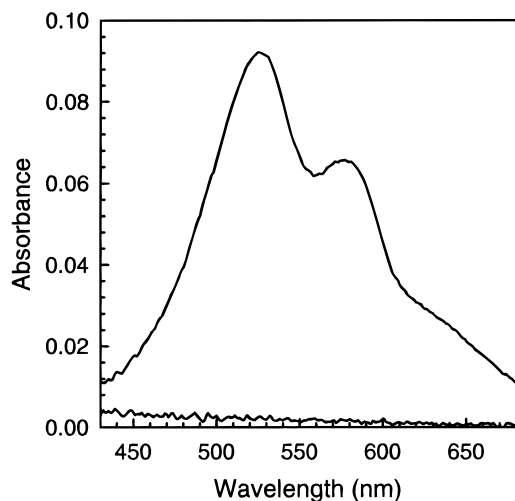


Figure 6. Absorption spectrum of the radical anion of imide **8** in benzonitrile containing 0.1 M tetrabutylammonium hexafluorophosphate generated electrochemically as described in the text.

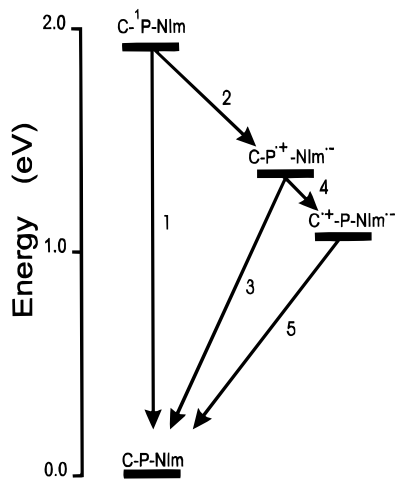


Figure 7. Relevant high-energy states of triad **4** and their interconversion pathways. The energies of the charge-separated states are estimated from cyclic voltammetric data for model compounds. Rate constants for the various processes are given in Table 2.

lead to concurrent formation of the carotenoid radical cation. Figure 3 shows that at 5 ps, no carotenoid radical cation absorption in the 930 nm region is detectable. In fact, as shown in the inset, the carotenoid radical cation absorption rises exponentially from zero with a time constant equal to the lifetime of the porphyrin first excited singlet state. Therefore, the porphyrin first excited singlet state gives rise to the charge-separated state by the two-step mechanism discussed above, and the carotenoid singlet state is not involved.

This conclusion is bolstered by the results of excitation at 556 nm, where the carotenoid moiety absorbs 43% of the excitation. The carotenoid radical cation absorption was again found to rise with the time constant of the decay of C-<sup>1</sup>P-NIm (99 ps), and no rise time corresponding to the 7.7 ns lifetime of <sup>1</sup>C-P-NIm was observed.

Finally, the transient absorption experiments on the nanosecond time scale demonstrate that excitation of the sample at 550 nm, where the carotenoid moiety absorbs approximately one-half of the light, produced a much lower quantum yield of the final C<sup>+</sup>-P-NIm<sup>-</sup> state than did excitation at 650 nm, where only the porphyrin absorbs. Thus, the porphyrin first excited singlet state is responsible for the vast majority of the long-lived charge-separated species.

It has been reported that excitation of the porphyrin moiety of triad **2** is followed by singlet-singlet energy transfer to the carotenoid, which then rapidly donates an electron to the imide to form the C<sup>+</sup>-P-Im<sup>-</sup> charge-separated state in a single electron-transfer step.<sup>27</sup> This is not the case with triad **4**. It is true that the porphyrin first excited singlet state of **6**, and therefore that of **4** as well, is quenched by the carotenoid. This quenching is presumably due to photoinduced electron transfer or singlet-singlet energy transfer. However, in **4**, the quantum yield of C-P<sup>+</sup>-NIm<sup>-</sup> from C-<sup>1</sup>P-NIm is 0.94, the yield of C<sup>+</sup>-P-NIm<sup>-</sup> is 0.33, and that of carotenoid quenching process is only 0.06. This alone requires that the majority of the C<sup>+</sup>-P-NIm<sup>-</sup> state be formed via the two-step route involving the porphyrin first excited singlet state. Charge separation from the carotenoid first excited singlet state produced by any energy transfer process may also be ruled out on the basis of the transient absorption experiments described above, which show that <sup>1</sup>C-P-NIm formed by direct excitation does not lead to detectable (>1%) formation of the carotenoid radical cation.

#### Solvent Dependence of Photoinduced Electron Transfer.

Perusal of Tables 1 and 2 shows that the rate of photoinduced electron transfer from the porphyrin first excited singlet state to NIm does not correlate in any simple way with the solvent dielectric constant. For example, photoinduced electron transfer is substantially faster in dichloromethane (dielectric constant = 8.9) than in benzonitrile (dielectric constant = 25.2). In this respect, the NIm acceptor parallels the behavior of quinone electron acceptors in porphyrin-quinone dyads, which also show unexpectedly large rates of photoinduced electron transfer in chlorinated solvents.<sup>39-43</sup> In contrast, the rates of photoinduced electron transfer between porphyrin moieties in porphyrin dyads correlate relatively smoothly with the solvent dielectric constant using the dielectric continuum model for solvent effects on thermodynamic driving force.<sup>44</sup>

**Charge Recombination.** The lifetimes of the C<sup>+</sup>-P-NIm<sup>-</sup> state in various solvents (Table 1) are roughly 4 orders of

magnitude longer than the lifetimes of the precursor  $C-P^{*+}-NIm^{*-}$  states. This tremendous lifetime extension is typical of triads, tetrads, and pentads that demonstrate multistep electron-transfer behavior.<sup>2,45-47</sup> Indeed, it is at the heart of the mechanism of action of natural photosynthetic reaction centers.

In principle, recombination of  $C^{*+}-P-NIm^{*-}$  may be either a single-step, direct electron transfer from the imide moiety to the carotenoid radical cation, or a two-step process. The two-step mechanism would involve, for example, slow, thermally activated recombination of  $C^{*+}-P-NIm^{*-}$  to  $C-P^{*+}-NIm^{*-}$  followed by rapid recombination of this species. The two-step process has been observed in a series of carotenoid-porphyrin-quinone triads,<sup>48</sup> whereas both kinds of behavior have been observed in previously studied carotenoid-porphyrin-imide triads such as **2** and **3**.<sup>32</sup>

The solvent dependence observed for charge recombination in **4** is qualitatively consistent with the two-step process. When solvent polarity is decreased, the energies of both the  $C^{*+}-P-NIm^{*-}$  and  $C-P^{*+}-NIm^{*-}$  states should increase because of loss of solvent dielectric stabilization of the charges. However, the increase should be smaller for  $C-P^{*+}-NIm^{*-}$  because of compensation due to increased mutual Coulombic stabilization of the adjacent ions in less polar solvents. This mutual effect is not as effective in  $C^{*+}-P-NIm^{*-}$ , where the charges are much farther apart. The net result of this is that the energy difference between  $C^{*+}-P-NIm^{*-}$  and  $C-P^{*+}-NIm^{*-}$  should decrease in nonpolar solvents, and this should speed up two-step charge recombination in less polar solvents, as is observed.

On the other hand, the energy of the final  $C^{*+}-P-NIm^{*-}$  state is expected to increase in nonpolar solvents and solvent reorganization energy to decrease; direct, single-step charge recombination in these solvents would likely occur in the inverted region of the Marcus equation.<sup>49,50</sup> Thus, the increase in driving force with decreasing solvent polarity should result in a decrease in the rate of charge recombination, in contrast to the observations. Further information on the charge recombination process must await studies of temperature dependence. However, it is interesting to note that charge recombination in triad **3** has been found to occur by the two-step mechanism at ambient temperatures.<sup>32</sup>

## Conclusions

In triad **4** photoinduced electron transfer originating from the porphyrin first excited singlet state has been found to initiate a two-step electron-transfer sequence that generates the  $C^{*+}-P-NIm^{*-}$  state in high yield. In benzonitrile, the  $C-P^{*+}-NIm^{*-}$  initial charge-separated state is produced with a quantum yield of 0.96, and  $C^{*+}-P-NIm^{*-}$  is formed with an overall yield of 0.33. The high yield, long lifetime, and high energy of the final  $C^{*+}-P-NIm^{*-}$  state in **4** suggests that triads of this general type may be useful in the design of more complex systems for harvesting photon energy or for optoelectronic applications.

In contrast to the results reported for closely related triads **2** and **3**,<sup>27</sup> photoinduced electron transfer from the carotenoid first excited singlet state to yield  $C^{*+}-P-NIm^{*-}$  was not detected in **4**. The reasons for this difference in behavior are not clear. It is unlikely that the fact that **4** features a 5,10 relationship of the carotenoid and acceptor on the porphyrin macrocycle whereas **2** and **3** have the 5,15 relationship is significant. Earlier studies have shown that carotenoid-porphyrin-quinone triads differing only in this respect have virtually identical photochemical properties.<sup>48,51</sup> Several factors may contribute to the difference in behavior. In the first place, the results for **4** do not completely rule out all photoinduced electron transfer from the carotenoid first excited singlet state; they simply require

that the quantum yield of any such process be exceedingly low relative to that of the two-step sequence. Since quantum yields were not reported in the earlier study,<sup>27</sup> direct comparison is not facile. An additional complicating factor is that in triads **2** and **3**, photoinduced electron transfer from  $C-P-NIm$  to yield  $C-P^{*+}-NIm^{*-}$  is very slow because the thermodynamic driving force is much lower than in triad **4**, and electronic coupling is likely not as great as in **4**. This makes it potentially easier to detect formation of the final charge-separated states by alternative routes. In addition, the porphyrin moiety used in the previous study differs from that in **4**, and thus, the energies of porphyrin excited states, porphyrin redox potentials, and the degree of electronic coupling of peripheral groups both to and through the porphyrin moiety will differ. Photoinduced electron transfer originating from carotenoid excited singlet states is certainly possible when it can compete with the very rapid relaxation of these states, and has been observed in other cases.<sup>52</sup>

Finally, the 4,5-dinitro-1,8-naphthalenedicarboximide moiety used as an electron acceptor in the molecules discussed here has been demonstrated to be an easily prepared, electrochemically reversible, one-electron acceptor with a convenient reduction potential. It is slightly more easily reduced than benzoquinone, and its radical anion has a characteristic absorption spectrum in the visible region. This imide should be useful in a variety of similar electron-acceptor applications.

## Experimental Section

**Synthesis.** The preparation of carotenoid **9** has been previously reported.<sup>51</sup>

**N-(4-Chlorophenyl)-4,5-dinitro-1,8-naphthalenedicarboximide (8).** A mixture of 100 mg (0.35 mmol) of 4,5-dinitro-1,8-naphthalenedicarboxylic anhydride<sup>53</sup> and 60 mg (0.47 mmol) of 4-chloroaniline in 5 mL of glacial acetic acid was refluxed overnight and then poured into 50 mL of water. The off-white precipitate was collected by filtration to yield 110 mg of crude product. This was recrystallized from chloroform and acetone to give 50 mg of white, silky crystalline imide (**8**) (36% yield), mp 296–298 °C. <sup>1</sup>H NMR (300 MHz, CDCl<sub>3</sub>): δ 7.26 (2H, d, *J* = 9 Hz, chlorophenyl), 7.56 (2H, d, *J* = 9 Hz, chlorophenyl), 8.51 (2H, d, *J* = 8 Hz, naphthyl), 8.87 (2H, d, *J* = 8 Hz, naphthyl). MS: *m/z* 397 (M<sup>+</sup>).

**5-(4-Acetamidophenyl)-10-(4-aminophenyl)-15,20-bis(4-methylphenyl)porphyrin (10).** A 57 mg portion (0.085 mmol) of 5,10-bis(4-aminophenyl)-15,20-bis(4-methylphenyl)porphyrin<sup>51</sup> and 38 mg of triethylamine were dissolved in 10 mL of chloroform. A solution of acetyl chloride in chloroform was slowly added dropwise with stirring. The reaction was monitored by thin-layer chromatography, and addition of acetyl chloride was stopped when a maximum amount of **10** was detected. The chloroform solution was washed with saturated aqueous sodium bicarbonate and water and dried with potassium carbonate. The solvent was removed by distillation at reduced pressure and the resulting material was chromatographed on silica gel (dichloromethane containing 5% methanol) to give 16 mg porphyrin **10** (26% yield). <sup>1</sup>H NMR (300 MHz, CDCl<sub>3</sub>): δ -2.76 (2H, s, pyrrole NH), 2.34 (3H, s, acetamido CH<sub>3</sub>), 2.70 (6H, s, Ar-CH<sub>3</sub>), 7.04 (2H, d, *J* = 8 Hz, 10Ar3,5-H), 7.49 (1H, s, amide NH), 7.54 (4H, d, *J* = 8 Hz, 15,20Ar3,5-H), 7.85 (2H, d, *J* = 8 Hz, 5-Ar3,5-H), 7.98 (2H, d, *J* = 8 Hz, 10Ar2,6-H), 8.08 (2H, d, *J* = 8 Hz, 15(20)Ar2,6-H), 8.09 (2H, d, *J* = 8 Hz, 20(15)Ar2,6-H), 8.15 (2H, d, *J* = 8 Hz, 5Ar2,6-H), 8.82–8.93 (8H, m, pyrrole H). MS: *m/z* 715 (M<sup>+</sup>).

**Dyad 5.** A mixture of 20 mg (0.028 mmol) of porphyrin **10** and 20 mg (0.069 mmol) of 4,5-dinitro-1,8-naphthalenedicarboxylic anhydride in 5 mL of glacial acetic acid was refluxed

gently for 1 h. The reaction mixture was then poured into 20 mL of water and extracted with three 10 mL portions of dichloromethane. The organic phase was washed with 5% aqueous sodium carbonate and with water and then dried over potassium carbonate. The solvent was removed by distillation at reduced pressure and the residue was chromatographed (silica gel, dichloromethane containing 5% methanol) to give 19.8 mg dyad **5** (72% yield).  $^1\text{H NMR}$  (500 MHz,  $\text{CDCl}_3$ ):  $\delta$  -2.69 (2H, s, pyrrole NH), 2.37 (3H, s, acetamido  $\text{CH}_3$ ), 2.71 (3H, s, 15(20)Ar- $\text{CH}_3$ ), 2.72 (3H, s, 20(15)Ar- $\text{CH}_3$ ), 7.54 (2H, d,  $J$  = 8 Hz, 15(20)Ar3,5-H), 7.57 (1H, s, amide NH), 7.57 (2H, d,  $J$  = 8 Hz, 20(15)Ar3,5-H), 7.67 (2H, d,  $J$  = 8 Hz, 10Ar3,5-H), 7.91 (2H, d,  $J$  = 8 Hz, 5Ar3,5-H), 8.10 (4H, d,  $J$  = 8 Hz, 15,20Ar2,6-H), 8.17 (2H, d,  $J$  = 8 Hz, 5Ar2,6-H), 8.41 (2H, d,  $J$  = 8 Hz, 10Ar2,6-H), 8.48 (2H, d,  $J$  = 8 Hz, naphthalimido H), 8.90 (2H, d,  $J$  = 8 Hz, naphthalimido H), 8.86–8.95 (8H, m, pyrrole H). MS:  $m/z$  985 ( $\text{M}^+$ ).

**Dyad 11.** A suspension of 11.8 mg (0.012 mmol) of dyad **5** in 3 mL of 6 N hydrochloric acid was heated on a steam bath for 1 h. After the reaction mixture was cooled to room temperature, the green solid was removed by filtration and dissolved in 20 mL of dichloromethane. The solution was washed with 5% sodium carbonate and water and dried with potassium carbonate, and the solvent was removed by distillation under reduced pressure. The purple residue was chromatographed (silica gel, dichloromethane containing 3% methanol) to give 8.7 mg of aminoporphyrin-imide dyad **11** (77% yield).  $^1\text{H NMR}$  (400 MHz,  $\text{CDCl}_3 + \text{CD}_3\text{OD}$ ):  $\delta$  2.72 (3H, s, 15(20)Ar- $\text{CH}_3$ ), 2.73 (3H, s, 20(15)Ar- $\text{CH}_3$ ), 7.11 (2H, d,  $J$  = 8 Hz, 5Ar3,5-H), 7.57 (2H, d,  $J$  = 8 Hz, 15(20)Ar3,5-H), 7.58 (2H, d,  $J$  = 8 Hz, 20(15)Ar3,5-H), 7.71 (2H, d,  $J$  = 8 Hz, 10Ar3,5-H), 8.02 (2H, d,  $J$  = 8 Hz, 5Ar2,6-H), 8.11 (4H, d,  $J$  = 8 Hz, 15,20Ar2,6-H), 8.44 (2H, d,  $J$  = 8 Hz, 10Ar2,6-H), 8.54 (2H, d,  $J$  = 8 Hz, naphthalimido H), 8.96 (2H, d,  $J$  = 8 Hz, naphthalimido H), 8.88 (8H, brs, pyrrole H). MS:  $m/z$  943 ( $\text{M}^+$ ).

**Triad 4.** A portion of 7'-apo-7'-(4-carboxyphenyl)- $\beta$ -carotene<sup>54</sup> (12.7 mg, 0.024 mmol) was dissolved in a mixture of 2 mL of dry toluene and 1 mL of dry pyridine. An excess of thionyl chloride was added and the mixture was stirred under a nitrogen atmosphere at room temperature for 10 min. All solvents and excess thionyl chloride were removed by vacuum distillation. The carotene acid chloride was redissolved in a mixture of 2 mL of dichloromethane and 0.5 mL of pyridine. The resulting solution was added to a dichloromethane solution containing 8.7 mg (0.0093 mmol) of aminoporphyrin-imide dyad **11**. The reaction mixture was stirred under a nitrogen atmosphere overnight at room temperature and worked up by washing with saturated sodium bicarbonate and water and drying with sodium sulfate. The solvent was removed by distillation at reduced pressure and the residue was chromatographed (silica gel, dichloromethane containing 3% methanol) to yield 6.1 mg of triad **4** (44% yield).  $^1\text{H NMR}$  (500 MHz,  $\text{CDCl}_3$ ):  $\delta$  -2.77 (2H, s, pyrrole NH), 1.04 (6H, s, Car 16- $\text{CH}_3$ , Car 17- $\text{CH}_3$ ), 1.42–1.51 (2H, m, Car 2- $\text{CH}_2$ ), 1.60–1.64 (2H, m, Car 3- $\text{CH}_2$ ), 1.72 (3H, s, Car 18- $\text{CH}_3$ ), 1.98 (3H, s, Car 19- $\text{CH}_3$ ), 1.99 (3H, s, Car 20- $\text{CH}_3$ ), 2.01 (3H, s, Car 20'- $\text{CH}_3$ ), 2.03 (2H, m, Car 4- $\text{CH}_2$ ), 2.10 (3H, s, Car 19'- $\text{CH}_3$ ), 2.71 (3H, s, 15(20)Ar- $\text{CH}_3$ ), 2.72 (3H, s, 20(15)Ar- $\text{CH}_3$ ), 6.1–7.1 (14H, m, Car = $\text{CH}$ -), 7.54–7.60 (4H, m, 15,20Ar3,5-H), 7.61 (2H, d,  $J$  = 8 Hz, Car 1',5'-H), 7.65 (2H, d,  $J$  = 8 Hz, 10Ar3,5-H), 7.99 (2H, d,  $J$  = 8 Hz, Car 2',4'-H), 8.06 (2H, d,  $J$  = 8 Hz, 5Ar3,5-H), 8.10 (4H, d,  $J$  = 8 Hz, 15,20Ar2,6-H), 8.17 (1H, s, amide NH), 8.23 (2H, d,  $J$  = 8 Hz, 5Ar2,6-H), 8.40 (2H, d,  $J$  = 8 Hz, 10Ar2,6-H), 8.47 (2H, d,  $J$  = 8 Hz, naphthalimido H), 8.89 (2H, d,  $J$  =

8 Hz, naphthalimido H), 8.89–8.96 (8H, m, pyrrole H). MS:  $m/z$  1459 ( $\text{M}^+$ ).

**Dyad 6.** A portion of 7'-apo-7'-(4-carboxyphenyl)- $\beta$ -carotene<sup>54</sup> (10 mg, 0.019 mmol) was dissolved in a mixture of 2 mL of dry toluene and 1 mL of dry pyridine. An excess of thionyl chloride was added and the mixture was stirred under a nitrogen atmosphere at room temperature for 10 min. All solvents and excess thionyl chloride were removed by vacuum distillation. The carotene acid chloride was redissolved in a mixture of 2 mL of dichloromethane and 0.5 mL of pyridine. The resulting solution was added to a dichloromethane solution containing 6.6 mg (0.0092 mmol) of aminoporphyrin **10**. The reaction mixture was stirred under a nitrogen atmosphere overnight at room temperature and worked up by washing with saturated sodium bicarbonate and water and drying with sodium sulfate. The solvent was removed by distillation at reduced pressure and the residue was chromatographed (silica gel, dichloromethane containing 3% methanol) to yield 10.2 mg of dyad **6** (90% yield).  $^1\text{H NMR}$  (500 MHz,  $\text{CDCl}_3$ ):  $\delta$  -2.77 (2H, s, pyrrole NH), 1.04 (6H, s, Car 16- $\text{CH}_3$ , Car 17- $\text{CH}_3$ ), 1.46–1.50 (2H, m, Car 2- $\text{CH}_2$ ), 1.60–1.65 (2H, m, Car 3- $\text{CH}_2$ ), 1.72 (3H, s, Car 18- $\text{CH}_3$ ), 1.98 (3H, s, Car 19- $\text{CH}_3$ ), 1.99 (3H, s, Car 20- $\text{CH}_3$ ), 2.01 (3H, s, Car 20'- $\text{CH}_3$ ), 2.03 (2H, m, Car 4- $\text{CH}_2$ ), 2.10 (3H, s, Car 19'- $\text{CH}_3$ ), 2.36 (3H, s, acetamido  $\text{CH}_3$ ), 2.71 (6H, s, 15,20Ar- $\text{CH}_3$ ), 6.1–7.1 (14H, m, Car = $\text{CH}$ -), 7.48 (1H, s, amide NH), 7.55 (4H, d,  $J$  = 8 Hz, 15,20Ar3,5-H), 7.63 (2H, d,  $J$  = 8 Hz, Car 1',5'-H), 7.89 (2H, d,  $J$  = 8 Hz, 10Ar3,5-H), 7.99 (2H, d,  $J$  = 8 Hz, Car 2',4'-H), 8.04 (2H, d,  $J$  = 8 Hz, 5Ar3,5-H), 8.09 (4H, d,  $J$  = 8 Hz, 15,20Ar2,6-H), 8.15 (1H, s, amide NH), 8.16 (2H, d,  $J$  = 8 Hz, 10Ar2,6-H), 8.22 (2H, d,  $J$  = 8 Hz, 5Ar2,6-H), 8.85–8.88 (8H, m, pyrrole H). MS:  $m/z$  1232 ( $\text{M}^+$ ).

**Absorption Spectrum of  $\text{NIm}^{\bullet-}$ .** A 50 mL glass cuvette was fitted for controlled-potential electrolysis; the three-electrode setup consisted of an optically transparent indium tin oxide (ITO) working electrode, a platinum foil counter electrode, and a silver/silver nitrate electrode to which all of the following potentials are referenced. To the cuvette was added 20 mL of a 0.1 M solution of tetrabutylammonium hexafluorophosphate in benzonitrile. This electrolyte solution was purged with high-purity nitrogen and exhibited no electroactivity within the usable range of the ITO electrode in this system (-1.2 to +0.6 V). Approximately 4 mg of *N*-(4-chlorophenyl)-4,5-dinitro-1,8-naphthalenedicarboximide (**8**) was dissolved in this solution. Cyclic voltammetry indicated a half-wave potential for reduction of **8** near -0.9 V. The cathodic and anodic sweeps exhibited significant dissimilarities in their wave shapes, indicating unique kinetics for each charge-transfer process. A small quantity of ferrocene was added to the cell in a subsequent cyclic voltammetry run after the spectrometric analysis, and this couple also displayed some quasi-reversibility in its waveforms. Thus, the anomalous kinetics may be attributable to the use of the semiconducting working electrode.

The cell was placed in the sample compartment of a Shimadzu UV2100U UV-vis spectrometer so that the probe beam passed through the solution normal to the ITO electrode. Changes in the absorbance of the cell were observed only when a potential below -0.8 V was applied to the working electrode. Figure 6 shows spectra recorded at 0.0 and -1.0 V; the latter is an average of four scans acquired once the cathodic current reached its diffusion-limited value (after about 20 s). Returning the applied potential to a value below  $E_{1/2}$  allowed eventual reoxidation of  $\text{NIm}^{\bullet-}$ , whereupon the spectrum matched that of the original solution at 0.0 V.

**Instrumental Techniques.** The  $^1\text{H NMR}$  spectra were

recorded on Varian Unity spectrometers at 300 or 500 MHz. Unless otherwise specified, samples were dissolved in deuteriochloroform with tetramethylsilane as an internal reference. Mass spectra were obtained on a Varian MAT 311 spectrometer operating in EI mode or a matrix-assisted laser desorption/ionization time-of-flight spectrometer (MALDI-TOF). Ultraviolet-visible spectra were measured on a Shimadzu UV2100U UV-vis spectrometer, and fluorescence spectra were measured on a SPEX Fluorolog using optically dilute samples and corrected.

Cyclic voltammetric measurements were carried out with a Pine Instrument Company Model AFRDE4 potentiostat. The electrochemical measurements were performed in benzonitrile at ambient temperatures with a glassy carbon working electrode, a Ag/Ag<sup>+</sup> reference electrode, and a platinum wire counter electrode. The electrolyte was 0.1 M tetra-*n*-butylammonium hexafluorophosphate, and ferrocene was employed as an internal reference redox system.

Fluorescence decay measurements were performed on  $\sim 1 \times 10^{-5}$  M solutions by the time-correlated single-photon counting method. The excitation source was a cavity-dumped Coherent 700 dye laser pumped by a frequency-doubled Coherent Antares 76s Nd:YAG laser.<sup>55</sup> The instrument response function was 35 ps, as measured at the excitation wavelength for each decay experiment with Ludox AS-40.

Transient absorption measurements on the picosecond time scale were made using the pump-probe technique. The sample was dissolved in purified solvent and the resulting solution was circulated by magnetic stirring in a cuvette having a 2 mm path length in the beam area. Excitation was at 590 nm with 150–200 fs, 30  $\mu$ J pulses at a repetition rate of 540 Hz. The signals from the continuum-generated white-light probe beam were collected by an optical spectrometric multichannel analyzer with a dual diode array detector head.<sup>56</sup>

Nanosecond transient absorption measurements were made with excitation from an Opotek optical parametric oscillator pumped by the third harmonic of a Continuum Surelight Nd:YAG laser. The pulse width was  $\sim 5$  ns, and the repetition rate was 10 Hz. The detection portion of the spectrometer has been described elsewhere.<sup>57</sup>

**Acknowledgment.** This work was supported by the National Science Foundation (CHE-9413084). This is Publication 323 from the ASU Center for the Study of Early Events in Photosynthesis.

## References and Notes

- Gust, D.; Moore, T. A. *Adv. Photochem.* **1991**, *16*, 1–65.
- Gust, D.; Moore, T. A.; Moore, A. L. *Acc. Chem. Res.* **1993**, *26*, 198–205.
- Wasielewski, M. R. *Chem. Rev. (Washington, D.C.)* **1992**, *92*, 435–461.
- Bixon, M.; Fajer, J.; Feher, G.; Freed, J. H.; Gamliel, D.; Hoff, A. J.; Levanon, H.; Mobius, K.; Nechushtai, R.; Norris, J. R.; Scherz, A.; Sessler, J. L.; Stehlik, D. *Isr. J. Chem.* **1992**, *32*, 449–455.
- Asahi, T.; Ohkohchi, M.; Matsusaka, R.; Mataga, N.; Zhang, R. P.; Osuka, A.; Maruyama, K. *J. Am. Chem. Soc.* **1993**, *115*, 5665–5674.
- Connolly, J. S.; Bolton, J. R. In *Photoinduced Electron Transfer, Part D*; Fox M. A., Channon M., Eds.; Elsevier: Amsterdam, 1988; pp 303–393.
- O'Neil, M. P.; Niemczyk, M. P.; Svec, W. A.; Gosztola, D.; Gaines, G. L., III; Wasielewski, M. R. *Science* **1992**, *257*, 63–65.
- Gust, D.; Moore, T. A.; Moore, A. L. *IEEE Eng. Med. Biol.* **1994**, *13*, 58–66.
- Debrezeny, M. P.; Svec, W. A.; Wasielewski, M. R. *Science* **1996**, *274*, 584–587.
- Gust, D.; Mathis, P.; Moore, A. L.; Liddell, P. A.; Nemeth, G. A.; Lehman, W. R.; Moore, T. A.; Bensasson, R. V.; Land, E. J.; Chachaty, C. *Photochem. Photobiol.* **1983**, *37S*, S46.
- Moore, T. A.; Gust, D.; Mathis, P.; Mialocq, J.-C.; Chachaty, C.; Bensasson, R. V.; Land, E. J.; Doizi, D.; Liddell, P. A.; Lehman, W. R.; Nemeth, G. A.; Moore, A. L. *Nature (London)* **1984**, *307*, 630–632.
- Liddell, P.; Macpherson, A. N.; Sumida, J.; Demanche, L.; Moore, A. L.; Moore, T. A.; Gust, D. *Photochem. Photobiol.* **1994**, *59S*, 36S.
- Liddell, P. A.; Sumida, J. P.; Macpherson, A. N.; Noss, L.; Seely, G. R.; Clark, K. N.; Moore, A. L.; Moore, T. A.; Gust, D. *Photochem. Photobiol.* **1994**, *60*, 537–541.
- Imahori, H.; Cardoso, S.; Tatman, D.; Lin, S.; Macpherson, A. N.; Noss, L.; Seely, G. R.; Sereno, L.; Chessa de Silber, J.; Moore, T. A.; Moore, A. L.; Gust, D. *Photochem. Photobiol.* **1995**, *62*, 1009–1014.
- Kuciauskas, D.; Lin, S.; Seely, G. R.; Moore, A. L.; Moore, T. A.; Gust, D.; Drovetskaya, T.; Reed, C. A.; Boyd, P. D. W. *J. Phys. Chem.* **1996**, *100*, 15926–15932.
- Drovetskaya, T.; Reed, C. A.; Boyd, P. D. W. *Tetrahedron Lett.* **1995**, *36*, 7971–7974.
- Imahori, H.; Hagiwara, K.; Akiyama, T.; Taniguchi, S.; Okada, T.; Sakata, Y. *Chem. Lett.* **1995**, 265–266.
- Imahori, H.; Sakata, Y. *Chem. Lett.* **1996**, 199–200.
- Cowan, J. A.; Sanders, J. K. M. *J. Chem. Soc., Perkin Trans. I* **1985**, 2435–2437.
- Harrison, R. J.; Pearce, B.; Beddard, G. S.; Cowan, J. A.; Sanders, J. K. M. *Chem. Phys.* **1987**, *116*, 429–448.
- Osuka, A.; Yamada, H.; Maruyama, K.; Mataga, N.; Asahi, T.; Yamazaki, I.; Nishimura, Y. *Chem. Phys. Lett.* **1991**, *181*, 419–426.
- Osuka, A.; Nagata, T.; Maruyama, K.; Mataga, N.; Asahi, T.; Yamazaki, I.; Nishimura, Y. *Chem. Phys. Lett.* **1991**, *185*, 88–94.
- Osuka, A.; Nagata, T.; Kobayashi, F.; Zhang, R. P.; Maruyama, K.; Mataga, N.; Asahi, T.; Ohno, T.; Nozaki, K. *Chem. Phys. Lett.* **1992**, *199*, 302–308.
- Ohkohchi, M.; Takahashi, A.; Mataga, N.; Okada, T.; Osuka, A.; Yamada, H.; Maruyama, K. *J. Am. Chem. Soc.* **1993**, *115*, 12137–12143.
- Osuka, A.; Zhang, R. P.; Maruyama, K.; Mataga, N.; Tanaka, Y.; Okada, T. *Chem. Phys. Lett.* **1993**, *215*, 179–184.
- Osuka, A.; Zhang, R. P.; Maruyama, K.; Ohno, T.; Nozaki, K. *Chem. Lett.* **1993**, 1727–1730.
- Osuka, A.; Yamada, H.; Maruyama, K.; Mataga, N.; Asahi, T.; Ohkouchi, M.; Okada, T.; Yamazaki, I.; Nishimura, Y. *J. Am. Chem. Soc.* **1993**, *115*, 9439–9452.
- Osuka, A.; Nakajima, S.; Maruyama, K.; Mataga, N.; Asahi, T.; Yamazaki, I.; Nishimura, Y.; Ohno, T.; Nozaki, K. *J. Am. Chem. Soc.* **1993**, *115*, 4577–4589.
- Maruyama, K.; Osuka, A.; Mataga, N. *Pure Appl. Chem.* **1994**, *66*, 867–872.
- Smirnov, S. N.; Braun, C. L.; Greenfield, S. R.; Svec, W. A.; Wasielewski, M. R. *J. Phys. Chem.* **1996**, *100*, 12329–12336.
- Greenfield, S. R.; Svec, W. A.; Gosztola, D.; Wasielewski, M. R. *J. Am. Chem. Soc.* **1996**, *118*, 6767–6777.
- Osuka, A.; Yamada, H.; Shinoda, T.; Nozaki, K.; Ohno, O. *Chem. Phys. Lett.* **1995**, *238*, 37–41.
- Osuka, A.; Marumo, S.; Maruyama, K.; Mataga, N.; Tanaka, Y.; Taniguchi, S.; Okada, T.; Yamazaki, I.; Nishimura, Y. *Bull. Chem. Soc. Jpn.* **1995**, *68*, 262–276.
- Osuka, A.; Marumo, S.; Wada, Y.; Yamazaki, I.; Yamazaki, T.; Shirakawa, Y.; Nishimura, Y. *Bull. Chem. Soc. Jpn.* **1995**, *68*, 2909–2915.
- Hung, S.-C.; Lin, S.; Macpherson, A. N.; DeGraziano, J. M.; Kerrigan, P. K.; Liddell, P. A.; Moore, A. L.; Moore, T. A.; Gust, D. *J. Photochem. Photobiol. A* **1994**, *77*, 207–216.
- Land, E. J.; Lexa, D.; Bensasson, R. V.; Gust, D.; Moore, T. A.; Moore, A. L.; Liddell, P. A.; Nemeth, G. A. *J. Phys. Chem.* **1987**, *91*, 4831–4835.
- Bonnett, R.; McGarvey, D. J.; Harriman, A.; Land, E. J.; Truscott, T. G.; Winfield, U.-J. *Photochem. Photobiol.* **1988**, *48*, 271–276.
- Wasielewski, M. R.; Liddell, P. A.; Barrett, D.; Moore, T. A.; Gust, D. *Nature (London)* **1986**, *322*, 570–572.
- Schmidt, J. A.; Siemiarz, A.; Weedon, A. C.; Bolton, J. R. *J. Am. Chem. Soc.* **1985**, *107*, 6112–6114.
- Bolton, J. R.; Ho, T.-F.; Liauw, S.; Siemiarz, A.; Wan, C. S.; Weedon, A. C. *J. Chem. Soc., Chem. Commun.* **1985**, 559–560.
- Liu, J.-Y.; Bolton, J. R. *J. Phys. Chem.* **1992**, *96*, 1718–1725.
- Liu, J.-Y.; Schmidt, J. A.; Bolton, J. R. *J. Phys. Chem.* **1991**, *95*, 6924–6927.
- Schmidt, J. A.; Liu, J.-Y.; Bolton, J. R.; Archer, M. D.; Gadzekpo, V. P. Y. *J. Chem. Soc., Faraday Trans. 1* **1989**, *85*, 1027–1041.
- DeGraziano, J. M.; Macpherson, A. N.; Liddell, P. A.; Noss, L.; Sumida, J. P.; Seely, G. R.; Lewis, J. E.; Moore, A. L.; Moore, T. A.; Gust, D. *New J. Chem.* **1996**, *20*, 839–851.
- Gust, D.; Moore, T. A.; Moore, A. L.; Lee, S.-J.; Bittersmann, E.; Luttrull, D. K.; Rehms, A. A.; DeGraziano, J. M.; Ma, X. C.; Gao, F.; Belford, R. E.; Trier, T. T. *Science* **1990**, *248*, 199–201.
- Gust, D.; Moore, T. A.; Moore, A. L.; Macpherson, A. N.; Lopez, A.; DeGraziano, J. M.; Gouni, I.; Bittersmann, E.; Seely, G. R.; Gao, F.; Nieman, R. A.; Ma, X. C.; Demanche, L.; Luttrull, D. K.; Lee, S.-J.; Kerrigan, P. K. *J. Am. Chem. Soc.* **1993**, *115*, 11141–11152.

- (47) Gust, D.; Moore, T. A. In *The Photosynthetic Reaction Center*; Norris, J. R., Deisenhofer, J., Eds.; Academic Press: New York, 1993; pp 419–464.
- (48) Gust, D.; Moore, T. A.; Makings, L. R.; Liddell, P. A.; Nemeth, G. A.; Moore, A. L. *J. Am. Chem. Soc.* **1986**, *108*, 8028–8031.
- (49) Marcus, R. A. *J. Chem. Phys.* **1956**, *24*, 966–978.
- (50) Marcus, R.; Sutin, N. *Biochim. Biophys. Acta* **1985**, *811*, 265–322.
- (51) Gust, D.; Moore, T. A.; Liddell, P. A.; Nemeth, G. A.; Makings, L. R.; Moore, A. L.; Barrett, D.; Pessiki, P. J.; Bensasson, R. V.; Rougée, M.; Chachaty, C.; de Schryver, F. C.; Van der Auweraer, M.; Holzwarth, A. R.; Connolly, J. S. *J. Am. Chem. Soc.* **1987**, *109*, 846–856.
- (52) Sereno, L.; Silber, J. J.; Otero, L.; Bohorquez, M. V.; Moore, A. L.; Moore, T. A.; Gust, D. *J. Phys. Chem.* **1996**, *100*, 814–821.
- (53) Bell, F. *J. Chem. Soc.* **1937**, 1952–1953.
- (54) Gust, D.; Moore, T. A.; Bensasson, R. V.; Mathis, P.; Land, E. J.; Chachaty, C.; Moore, A. L.; Liddell, P. A.; Nemeth, G. A. *J. Am. Chem. Soc.* **1985**, *107*, 3631–3640.
- (55) Gust, D.; Moore, T. A.; Luttrull, D. K.; Seely, G. R.; Bittersmann, E.; Bensasson, R. V.; Rougée, M.; Land, E. J.; de Schryver, F. C.; Van der Auweraer, M. *Photochem. Photobiol.* **1990**, *51*, 419–426.
- (56) Lin, S.; Chiou, H.-C.; Kleinherenbrink, F. A. M.; Blankenship, R. E. *Biophys. J.* **1994**, *66*, 437–445.
- (57) Davis, F. S.; Nemeth, G. A.; Anjo, D. M.; Makings, L. R.; Gust, D.; Moore, T. A. *Rev. Sci. Instrum.* **1987**, *58*, 1629–1631.